

Boron-oxygen defect in Czochralski-silicon co-doped with gallium and boron

M. Forster,^{1,2,3,a)} E. Fourmond,² F. E. Rougieux,³ A. Cuevas,³ R. Gotoh,⁴ K. Fujiwara,⁴ S. Uda,⁴ and M. Lemiti²

¹APOLLON SOLAR, 66 cours Charlemagne, 69002 Lyon, France

²INSA de LYON, INL, 7 av. J. Capelle, 69621 Villeurbanne Cedex, France

³School of Engineering, College of Engineering and Computer Science, The Australian National University, Canberra ACT 0200, Australia

⁴Institute for Material Research, Tohoku University, 2-1-1 Katahira, Aoba-ku, Sendai 980-8577, Japan

(Received 20 November 2011; accepted 10 January 2012; published online 27 January 2012)

We study the boron-oxygen defect in Si co-doped with gallium and boron with the hole density 10 times higher than the boron concentration. Instead of the linear dependence of the defect density on the hole density observed in boron and phosphorus compensated silicon, we find a proportionality to the boron concentration. This indicates the participation of substitutional, rather than interstitial, boron in the defect complex. The measured defect formation rate constant is proportional to the hole density squared, which gives credit to latent defect models against defect reactions limited by the diffusion and trapping of oxygen dimers by boron atoms. © 2012 American Institute of Physics. [doi:10.1063/1.3680205]

A degradation of the minority-carrier lifetime is known to occur in boron (B)-doped and oxygen (O)-containing crystalline silicon (Si) under illumination or carrier injection. Therefore, solar cells made of B-doped Czochralski (Cz)-Si or cast multi-crystalline (mc)-Si suffer from a loss of conversion efficiency of up to 10% relative. This issue has to be addressed with particular care in the case of Cz-Si containing high O concentrations or low-cost upgraded-metallurgical grade (Ref. 1) (UMG)-Si which usually contains larger B concentrations than standard Siemens purified Si. Since 2004 (Ref. 2) and until very recently, the observed degradation was believed to be due to the formation of a complex made up of one *substitutional* B atom (B_s) and one *interstitial* O dimer (O_{2i}). This defect model was proposed after the observation that the saturated (i.e., after complete degradation) effective defect density $N_{t,sat}^*$ exhibits a linear dependence on B_s concentration $[B]$ and a quadratic dependence on *interstitial* O concentration $[O_i]$. However, recent measurements made on B and phosphorus (P) co-doped *p*-type Si (Refs. 3 and 4) showed that $N_{t,sat}^*$ was proportional to the hole density p_0 (i.e., to the net dopant density $N_A - N_D$) rather than to the total boron concentration $[B]$. Note that this observation was made possible in Si co-doped with B and P because p_0 is, in such material, systematically below $[B]$ whereas it is almost equal to $[B]$ in uncompensated B-doped Si. This finding was initially explained by the existence of B-P pairs in compensated Si resulting in a decrease of available B_s atoms for B_sO_{2i} complex formation.³ However, the existence of such B-P pairs in large proportion was later shown to be very doubtful^{5,6} and thus unable to explain the observed reduction of $N_{t,sat}^*$ in compensated *p*-type Si.

In the light of those observations, Voronkov and Falster⁷ proposed a model consisting of a latent defect made of one *interstitial* boron atom B_i and one oxygen dimer O_{2i} . The linear dependence of $N_{t,sat}^*$ on p_0 is thereby explained by the proportionality of the solubility N_{Bi} of positively charged B_i^+ in *p*-type Si to the free hole density, during the last stage

of crystal cooling. The degradation is proposed to result from a change of the configuration of the defect triggered by the injection of excess carriers.

On the other hand, it is well-known that light-induced minority-carrier lifetime degradation does not take place in electronic-grade (EG)-Si doped with only gallium (Ga). This implies that either no complex can form between Ga atoms and O_{2i} (Refs. 2 and 8) or such complex is electrically inactive.⁹ In Ga and B co-doped Cz-Si samples of the same total doping $p_0 = [B] + [Ga] \approx 1.5 \times 10^{16} \text{ cm}^{-3}$, Arivanandhan *et al.*¹⁰ measured lower lifetime after degradation in samples containing higher $[B]$. This result might lead one to question Voronkov and Falster's model which would expect, in Si containing B, the amplitude of the degradation to be proportional to p_0 and independent on $[B]$. Arivanandhan's study was, however, based on minority-carrier lifetime measurements on samples with no surface passivation and in which $[O_i]$ was not measured, assuming the latter to be the same in all samples. Given the quadratic dependence of $N_{t,sat}^*$ on $[O_i]$, an experimental measurement of $[O_i]$ is, however, essential. Moreover, the degraded lifetime was measured after only 120 min light-soaking which is *a priori* insufficient to ensure complete degradation.

In this work, we focus on the boron-oxygen (BO) defect in Si co-doped with Ga and B in which $p_0 > [B]$. We determine the saturated defect density and formation rate and study their dependences on $[B]$ and p_0 . The aim of the present work is to check whether the presence of Ga in Si co-doped with B impacts on the formation of the BO defect and to verify if experimental results are consistent with a recently proposed defect model⁷ based on measurements in B-doped and B and P co-doped Si.

For that purpose, samples were selected at different heights (20%, 30%, and 40%) of a Cz-Si crystal of 50–70 mm in diameter, grown from a melt doped with $1.47 \times 10^{15} \text{ cm}^{-3}$ of B and $1.67 \times 10^{18} \text{ cm}^{-3}$ of Ga. These samples, together with B-doped and Ga-doped Cz-Si control samples, were first subjected to a phosphorus-diffusion gettering at 820 °C to dissolve oxygen-related thermal donors (TDs) and eliminate metallic impurities. This ensures that there is no or very little

^{a)}Author to whom correspondence should be addressed. Electronic mail: forster@apollonsolar.com.

impact of Fe-B or Fe-Ga pairs during the degradation experiment. Then, samples were subsequently acid etched to remove the diffused layers and the saw damage, RCA cleaned and coated on both sides at low temperature (400 °C) with PECVD hydrogenated silicon-nitride ($\text{SiN}_x\text{:H}$) layers in order to ensure a good surface passivation.¹¹ The samples' thicknesses, after acid etch, were in the range 130–560 μm . The minority-carrier lifetime $\tau(t)$ was then measured using the quasi-steady-state photoconductance (QSSPC) technique (Ref. 12) immediately after annihilation of the boron-oxygen defect by a 30 min annealing at 200 °C in the dark ($t=0$), and after different degradation times t under a 10 mW/cm² light-soaking at a temperature of 25–27 °C. Samples were carefully protected from light-exposure between annealing and the initial minority-carrier lifetime measurement to ensure that no BO defects were generated before the measurement of $\tau(0)$. The minority-carrier lifetime degraded under illumination in all the samples except for the Ga-doped Si one, in which it remained stable (Fig. 1). This proves that the surface passivation quality of the $\text{SiN}_x\text{:H}$ layer did not change throughout the experiment. The observed degradation in samples containing B can thus be attributed to a decrease of the bulk lifetime.

$\text{SiN}_x\text{:H}$ layers were then etched off in hydrofluoric acid and $[\text{O}_i]$ was determined by Fourier transform infrared spectroscopy (FTIR) to be in the range $[\text{O}_i] = (6 \pm 1) \times 10^{17} \text{ cm}^{-3}$ to $(11 \pm 2) \times 10^{17} \text{ cm}^{-3}$. Carbon is also known to affect the defect density,² presumably by capturing O_{2i} .¹³ Its concentration was measured in our samples by FTIR to be comprised in the narrow range $[\text{C}] = (7 \pm 1) \times 10^{16} \text{ cm}^{-3}$ to $(9 \pm 2) \times 10^{16} \text{ cm}^{-3}$ and should thus not have a significant influence in the present study. In each sample, the carrier density p_0 is deduced from the resistivity measured with a four-point probe, in the range 0.7–10.4 Ωcm . In samples doped with B only, $[\text{B}]$ is taken as equal to p_0 , assuming complete dopant ionization. This assumption is valid since only samples with $[\text{B}]$ lower than $2 \times 10^{16} \text{ cm}^{-3}$ are considered in this work.¹⁴ In samples co-doped with Ga and B, $[\text{B}]$ is calculated from the sample's position in the crystal and the initial concentrations in the Si melt using the Scheil equation. In our samples, it lies in the range $[\text{B}] = (1.2 \pm 0.5) \times 10^{15} \text{ cm}^{-3}$ to $(1.3 \pm 0.9) \times 10^{15} \text{ cm}^{-3}$. Note that the high segregation coefficient of B in Si ($k_B = 0.8$) means that its concentration varies along the ingot much less than the concentration of Ga. In addition, no significant evaporation of B from the melt is expected to occur. Hence, the B concentration at a given height of the ingot can be determined with an accuracy that is sufficient for the purposes of the present study. These co-doped samples present the advantage for this study that they contain more Ga than B and therefore p_0 is about 10 times higher than $[\text{B}]$. This will enable us to clearly establish if the defect density's linear dependence on p_0 , observed in compensated Si in which $p_0 < [\text{B}]$, is still valid when $p_0 > [\text{B}]$.

After a degradation time t , the effective defect density $N_t^*(t)$ is calculated with the following expression,

$$N_t^*(t) = \frac{1}{\tau_{\text{LID}}} = \frac{1}{\tau(t)} - \frac{1}{\tau(0)}, \quad (1)$$

$\tau(t)$ being the minority-carrier lifetime measured at a fixed excess-carrier injection Δn equal to 10% of the carrier den-

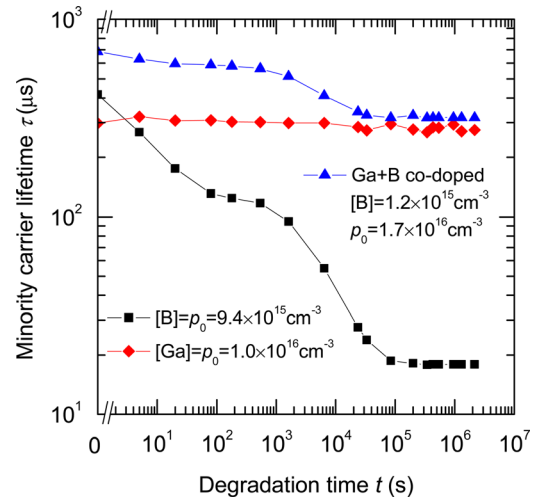


FIG. 1. (Color online) Minority-carrier lifetime measured in B-doped and Ga-doped controls and in Si co-doped with Ga and B as a function of time under illumination at 10 mW/cm². Lines are guides to the eye.

sity p_0 after illumination for a duration t . The evolution of $N_t^*(t)$ with illumination time can be fitted, as previously reported,³ with

$$N_t^*(t) = N_{\text{fast}}^* + N_{\text{t,sat}}^* \cdot (1 - \exp(-R_{\text{gen}} \cdot t)), \quad (2)$$

in which N_{fast}^* accounts for a fast initial degradation occurring during the first few seconds of light exposure which can be observed in Fig. 1. Since this fast degradation has a very small impact on the final degraded τ , we only focus on the slow-forming defect by studying its saturated effective density $N_{\text{t,sat}}^*$ and formation rate constant R_{gen} .

It is well known that $N_{\text{t,sat}}^*$ displays a quadratic dependence on $[\text{O}_i]$. This dependence is thought to be due to the participation of oxygen dimers² which are themselves present in a concentration proportional to $[\text{O}_i]$ squared.¹³ Hence, small variations in $[\text{O}_i]$ from sample to sample can lead to significant variations in $N_{\text{t,sat}}^*$ even for equal doping levels. Since we intend to study the impact of dopant concentration on the defect density and the nature of the B atom involved in the complex, a more relevant parameter to focus on is $N_{\text{BC}} = N_{\text{t,sat}}^*/[\text{O}_i]$.² This oxygen-normalized parameter reflects the influence of defect components (such as $[\text{B}]$ or p_0) not directly related to $[\text{O}_i]$.

The relative defect density N_{BC} measured for three samples co-doped with Ga and B and three B-doped control samples is plotted in Fig. 2 as a function of p_0 and $[\text{B}]$. For comparison, we have also plotted a linear regression of experimental data points from Schmidt and Bothe² obtained on uncompensated B-doped Cz-Si samples. A reduction of the BO defect density by about a factor of 2 was found by the same authors in P-diffused Si as compared to as-cut Si.¹⁵ Since our samples underwent a phosphorus-diffusion, whereas the samples from Ref. 2 did not, we have corrected the linear fit from Ref. 2 by dividing the effective defect density by 2, in order to be able to compare it with our measurements. We have also plotted for comparison two points from Lim *et al.*⁴ on P-diffused B and P compensated p -type Si. These two points correspond to the seed and tail ends of the ingot studied in their paper, for which the measured value of

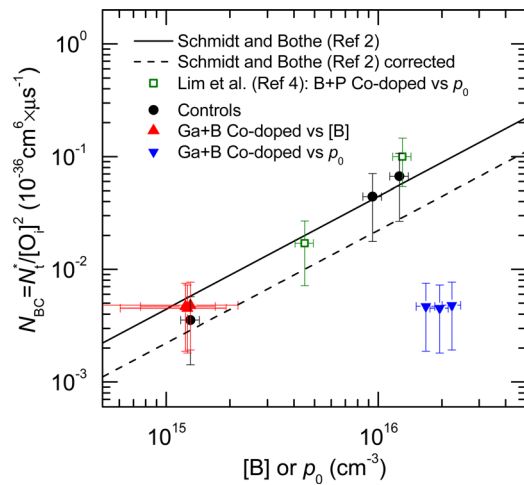


FIG. 2. (Color online) Relative saturated defect density plotted in B-doped controls and in Si co-doped with B and Ga as a function of the B concentration or the carrier density. Solid line is a fit to experimental data on B-doped Si from Ref. 2. Dashed line corresponds to the same fit divided by a correction factor of 2 to account for the defect density reduction expected in P-diffused Si. Open symbols correspond to effective defect density from Ref. 4 measured in P-diffused B and P compensated Si and plotted as a function of p_0 .

[O_i] was reported. As can be seen in Fig. 2, B-doped controls measured in the present work agree well with the previously measured defect density, which supports the validity of our experimental setup. In samples co-doped with Ga and B, however, N_{BC} is reduced by more than one order of magnitude compared to B-doped Si when plotted against p_0 . On the other hand, it scales well with B-doped Si when plotted as a function of [B]. Note that the drastic reduction of N_{BC} compared to the linear dependence on p_0 is only observable in these samples because [B] is about 10 times lower than p_0 due to the high concentration of Ga. We conclude from this result that in Si co-doped with B and Ga, the defect density is not related to p_0 but is, instead, proportional to [B]. This gives a general picture of the defect in which its density is proportional to $p_0 = N_A - N_D$ when $p_0 < [B]$ (i.e., when co-doped with P (Refs. 3 and 4)) and to [B] when $p_0 > [B]$ (i.e., when co-doped with Ga). Voronkov and Falster's model⁷ fails to describe the present result, since the concentration of dissolved interstitial B_i involved in that defect model is believed to be proportional to p_0 and independent on [B]. Instead, the proportionality with [B], found in our experiments, indicates the participation of substitutional B_s in the defect formation. The reduction of the defect density observed in Si compensated with P as compared to the expected linear dependence on [B] remains, however, to be explained.

One could also imagine that the defect is made of B_i, according to Voronkov and Falster's model, but that either one of the two densities of B_i or O_{2i} is strongly affected by the presence of Ga. For example, the formation of B_iGa_s or Ga_sO_{2i} pairs during the cooling of samples after phosphorus-diffusion is conceivable. No indication of the existence of such complexes has, however, been reported yet. Further investigation would be necessary to assess if they would be stable enough to reduce either concentrations of B_i or O_{2i} to such an extent that the BO defect density would decrease by more than one order of magnitude, as it is observed in this work.

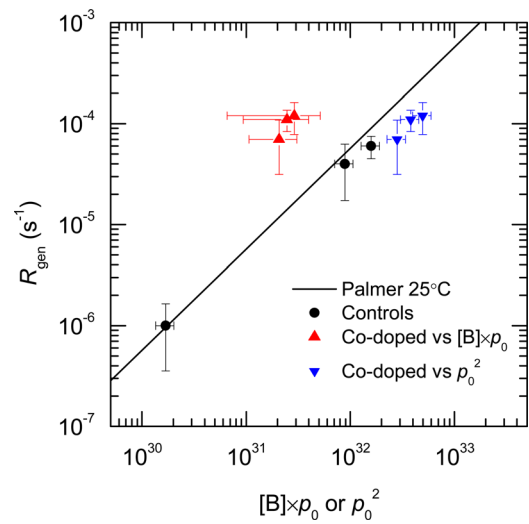


FIG. 3. (Color online) Defect formation rate constant plotted as a function of p_0^2 or $[B] \times p_0$, in B-doped controls and Si co-doped with B and Ga. Solid line represents R_{gen} at 25 °C as calculated with Palmer's model.

The formation rate constant R_{gen} of the slow forming BO defect can also be informative to understand the genesis of the defect. Its value, extracted from the fit of equation (2) to the measured $N_t^*(t)$, is plotted in Fig. 3 against p_0^2 and $p_0 \times [B]$. Fig. 3 also depicts R_{gen} calculated with Palmer's model, which fits previous experimental data in uncompensated B-doped Si.¹⁶ As can be seen, R_{gen} measured in the B-doped controls agrees well with Palmer's model, which again proves the validity of our experimental setup.

Depending on the defect formation mechanism, the formation rate constant R_{gen} is believed to depend either on p_0^2 or on $p_0 \times [B]$. A linear dependence on p_0^2 is expected from the reconstruction of a latent defect,⁷ whereas a defect reaction involving the diffusion of mobile O_{2i} under illumination should result in our samples in a linear dependence on $p_0 \times [B]$,¹⁶ since the B-related component of the defect was shown to be proportional to [B]. In the co-doped samples measured in this work, R_{gen} scales well with uncompensated Si when plotted against p_0^2 but shows significant deviation when plotted against $p_0 \times [B]$. It is worth noting that in *p*-type Si co-doped with B and P, R_{gen} is also proportional to p_0^2 , despite the fact that $p_0 < [B]$.^{3,4} It seems, therefore, that whatever the ratio between p_0 and [B], R_{gen} is always determined by p_0^2 and independent on [B]. This result therefore supports the version of the defect model in which it is activated by the reconfiguration of its latent state into a recombination-active form. Note that this does not contradict our previous conclusion that B_s is involved in the defect complex instead of B_i. The latent character of the complex does not imply a specific composition; the existence of a latent B_sO_{2i} defect that would form during Si cooling is possible.

In summary, we have measured the effective BO defect density in Si co-doped with B and Ga to be significantly reduced compared to the linear dependence on p_0 expected by the model recently proposed by Voronkov and Falster.⁷ Instead, the defect density in samples studied in this work shows a good agreement with a linear dependence on [B]. This result could be explained either by the involvement of

B_s instead of B_i in the defect or by the reduction of the density of B_i or O_{2i} due to the presence of Ga. In any case, the implications of this result for solar cells are positive. For example, it shows that the addition of Ga during crystallization of UMG-Si, used to control the Si doping uniformity,¹⁷ does not lead, as would be expected by Voronkov and Falster's model, to a stronger degradation. Finally, the measured linear dependence of R_{gen} on p_0^2 supports a model for the defect formation based on the activation of a latent defect, rather than due to the diffusion and trapping of O_{2i} .

¹J. Kraiem, B. Drevet, F. Cocco, N. Enjalbert, S. Dubois, D. Camel, D. Grosset-Bourbange, D. Pelletier, T. Margaria, and R. Einhaus, in *Proceedings 35th IEEE Photovoltaic Specialists Conference, Hawaii* (IEEE, New York, 2010).

²J. Schmidt and K. Bothe, *Phys. Rev. B* **69**, 024107 (2004).

³D. Macdonald, F. Rougieux, A. Cuevas, B. Lim, J. Schmidt, M. D. Sabatino, and L. J. Geerligs, *J. Appl. Phys.* **105**, 093704 (2009).

⁴B. Lim, F. Rougieux, D. Macdonald, K. Bothe, and J. Schmidt, *J. Appl. Phys.* **108**, 103722 (2010).

⁵D. Macdonald, A. Liu, F. Rougieux, A. Cuevas, B. Lim, J. Schmidt, M. D. Sabatino, and L. J. Geerligs, in *Proceedings of the 24th European Photovoltaic Solar Energy Conference, Hamburg, Germany* (WIP, Munich, 2009), p. 877.

⁶T. Schutz-Kuchly, J. Veirman, S. Dubois, and D. R. Heslinga, *Appl. Phys. Lett.* **96**, 093505 (2010).

⁷V. V. Voronkov and R. Falster, *J. Appl. Phys.* **107**, 053509 (2010).

⁸M. Sanati and S. K. Estreicher, *Physica B* **376–377**, 133 (2006).

⁹J. Adey, R. Jones, D. W. Palmer, P. R. Briddon, and S. Öberg, *Phys. Rev. Lett.* **93**, 055504 (2004).

¹⁰M. Arivanandhan, R. Gotoh, K. Fujiwara, and S. Uda, *J. Appl. Phys.* **106**, 013721 (2009).

¹¹J.-F. Lelièvre, E. Fourmond, A. Kaminski, O. Palais, D. Ballutaud, and M. Lemiti, *Sol. Energy Mater. Solar Cells* **93**, 1281 (2009).

¹²R. A. Sinton and A. Cuevas, *Appl. Phys. Lett.* **69**, 2510 (1996).

¹³L. I. Murin, T. Hallberg, V. P. Markevich, and J. L. Lindström, *Phys. Rev. Lett.* **80**, 93 (1998).

¹⁴P. P. Altermatt, A. Schenk, B. Schmithusen, and G. Heiser, *J. Appl. Phys.* **100**, 113715 (2006).

¹⁵K. Bothe, R. Sinton, and J. Schmidt, *Prog. Photovoltaics* **13**, 287 (2005).

¹⁶D. W. Palmer, K. Bothe, and J. Schmidt, *Phys. Rev. B* **76**, 035210 (2007).

¹⁷M. Forster, E. Fourmond, R. Einhaus, H. Lauvray, J. Kraiem, and M. Lemiti, *Phys. Status Solidi C* **8**, 678 (2011).